

Deep-ultraviolet and visible dual-band photodetectors by integrating Chlorin e6 with Ga_2O_3

Yue Zhao(赵越), Jin-Hao Zang(臧金浩), Xun Yang(杨珣), Xue-Xia Chen(陈雪霞), Yan-Cheng Chen(陈彦成), Kai-Yong Li(李凯永), Lin Dong(董林), and Chong-Xin Shan(单崇新)

Citation: Chin. Phys. B, 2021, 30 (**7**): 078504. DOI: 10.1088/1674-1056/abf91c
Journal homepage: http://cpb.iphy.ac.cn; http://iopscience.iop.org/cpb

What follows is a list of articles you may be interested in

Cathodic shift of onset potential on TiO_2 nanorod arrays with significantly enhanced visible light photoactivity via nitrogen/cobalt co-implantation

Xianyin Song(宋先印), Hongtao Zhou(周洪涛), and Changzhong Jiang(蒋昌忠)
Chin. Phys. B, 2021, 30 (**5**): 058505. DOI: 10.1088/1674-1056/abee07

Microstructure, optical, and photoluminescence properties of β-Ga_2O_3 films prepared by pulsed laser deposition under different oxygen partial pressures

Rui-Rui Cui(崔瑞瑞), Jun Zhang(张俊), Zi-Jiang Luo(罗子江), Xiang Guo(郭祥), Zhao Ding(丁召), and Chao-Yong Deng(邓朝勇)
Chin. Phys. B, 2021, 30 (**2**): 028505. DOI: 10.1088/1674-1056/abc164

Review of deep ultraviolet photodetector based on gallium oxide

Yuan Qin(覃愿), Shibing Long(龙世兵), Hang Dong(董航), Qiming He(何启鸣), Guangzhong Jian(菅光忠), Ying Zhang(张颖), Xiaohu Hou(侯小虎), Pengju Tan(谭鹏举), Zhongfang Zhang(张中方), Hangbing Lv(吕杭炳), Qi Liu(刘琦), Ming Liu(刘明)
Chin. Phys. B, 2019, 28 (**1**): 018501. DOI: 10.1088/1674-1056/28/1/018501

An improved design for AlGaN solar-blind avalanche photodiodes with enhanced avalanche ionization

Yin Tang(汤寅), Qing Cai(蔡青), Lian-Hong Yang(杨莲红), Ke-Xiu Dong(董可秀), Dun-Jun Chen(陈敦军), Hai Lu(陆海), Rong Zhang(张荣), You-Dou Zheng(郑有炓)
Chin. Phys. B, 2017, 26 (**3**): 038503. DOI: 10.1088/1674-1056/26/3/038503

Performance improvement of AlGaN-based deep ultraviolet light-emitting diodes with double electron blocking layers

Cheng Zhang(张诚), Hui-Qing Sun(孙慧卿), Xu-Na Li(李旭娜), Hao Sun(孙浩), Xuan-Cong Fan(范宣聪), Zhu-Ding Zhang(张柱定), Zhi-You Guo(郭志友)
Chin. Phys. B, 2016, 25 (**2**): 028501. DOI: 10.1088/1674-1056/25/2/028501

Deep-ultraviolet and visible dual-band photodetectors by integrating Chlorin e6 with Ga_2O_3

Yue Zhao(赵越), Jin-Hao Zang(臧金浩), Xun Yang(杨珣)†, Xue-Xia Chen(陈雪霞), Yan-Cheng Chen(陈彦成), Kai-Yong Li(李凯永), Lin Dong(董林)‡, and Chong-Xin Shan(单崇新)§

Key Laboratory of Materials Physics, Ministry of Education, Henan Key Laboratory of Diamond Optoelectronic Materials and Devices, School of Physics and Microelectronics, Zhengzhou University, Zhengzhou 450052, *China*

(Received 23 February 2021; revised manuscript received 30 March 2021; accepted manuscript online 19 April 2021)

Gallium oxide (Ga_2O_3) is a promising material for deep-ultraviolet (DUV) detection. In this work, Chlorin e6 (Ce6) has been integrated with Ga_2O_3 to achieve a DUV and visible dual-band photodetector, which can achieve multiple target information and improve the recognition rate. The photodetector shows two separate response bands at 268 nm and 456 nm. The DUV response band has a responsivity of 9.63 A/W with a full width at half maximum (FWHM) of 54.5 nm; the visible response band has a responsivity of 1.17 A/W with an FWHM of 45.3 nm. This work may provide a simple way to design and fabricate photodetectors with dual-band response.

Keywords: deep ultraviolet, visible, dual-band photodetector, Ga_2O_3

PACS: 85.60.Gz, 07.60.Rd, 61.72.uj **DOI:** 10.1088/1674-1056/abf91c

1. Introduction

Photodetecotors, which convert light to electrical signals, are one of the core components of information technology, such as biomedical imaging systems, ultraviolet astronomy, wide spectral switches, memory storage, *etc*.[1,2] To achieve multiple target information and improve the recognition rate, photodetectors that response in different bands are usually integrated. In order to simplify the detection system and reduce the false alarm rate, it is indispensable to realize multiple band accurate detection using a single photodetector, that is dual-band photodetector.[3,4] Dual-band photodetector can be applied in various fields, such as identification of objects, imaging under varying atmospheric conditions, machine vision, *etc*.[5] In particular, dual-band photodetectors working in deep-ultraviolet (DUV) and visible regions[6] are very attractive for applications in space research and environmental and biological research.[7,8] However, the report on the DUV-visible dual-band photodetectors is still rare to date.

Gallium oxide (Ga_2O_3) has become a promising material in DUV detection due to its wide band-gap of 4.9 eV, large absorption coefficient, high electron mobility, and good physical and chemical stability.[9] While Ga_2O_3 shows only a narrow detection band in the DUV region. One way to realize a DUV and visible dual-band photodetector is to integrate Ga_2O_3 with another material that responses to visible light.[10,11] Quantum dots and organic dyes, which show high light absorption efficiency, have been utilized to enhance the light absorption and spectral selectivity of photodetectors.[12] Especially, Ce6, which is a derivative of natural chlorophyll, shows highly spectrum-selective absorption in the visible region.[13] Owing to the excellent optical properties with no solubility issues, Ce6 has been widely used in dye-sensitized solar cell and photodynamic therapy.[13,14] Therefore, it is expected that a DUV and visible dual-band photodetector can be realized by combing Ga_2O_3 with Ce6. However, none such report can be found up to date.

In this work, a DUV and visible dual-band photodetector has been developed based on β-Ga_2O_3/MoS_2/Ce6 structures. The β-Ga_2O_3/MoS_2/Ce6 photodetector shows two separate response bands at 268 nm and 456 nm, which can be attributed to light absorption of the β-Ga_2O_3 and Ce6 layer, respectively. The response peak at 268 nm has a maximum responsivity of 9.63 A/W with a full width at half maximum (FWHM) of 54.5 nm. The response peak at 456 nm has a maximum responsivity of 1.17 A/W with an FWHM of 45.3 nm. This work may provide a sample way to design and fabricate photodetectors with multi-band response, which can improve the detection accuracy.

2. Experimental details

The Ga_2O_3 films were grown on *c*-plane sapphire substrates using a plasma enhanced chemical vapor deposition (PECVD) system.[15] High-purity oxygen (O_2) and triethylgallium (TEGa) were used as the precursors for the growth, while nitrogen (N_2) was used to lead the reactant gas into the growth chamber. During the growth, the substrate temperature was kept at 750 °C, and the pressure of the chamber was fixed at 1.1 mbar (1 bar = 10^5 Pa). The N_2 and O_2 flow rates were maintained at 10 sccm and 15 sccm, respectively.

†Corresponding author. E-mail: yangxun9013@163.com
‡Corresponding author. E-mail: ldong@zzu.edu.cn
§Corresponding author. E-mail: cxshan@zzu.edu.cn

© 2021 Chinese Physical Society and IOP Publishing Ltd

Molybdenum trioxide (MoO_3, 99.99%) and sulfur (S, 99.5%) were employed as the precursors to synthesize the MoS_2 through chemical vapor deposition (CVD) procedure. Previous to the growth, Si substrate with 300-nm SiO_2 was cleaned with acetone, alcohol and deionized water for 10 min, respectively. Then an aluminum boat with 5-mg MoO_3 powder (99.95%, Alfa Aesar) was placed into the quartz tube and located at the high temperature region of the furnace. The cleaned substrate was placed face down upon the quartz boat. Simultaneously, another quartz boat carrying 150-mg sulfur (99.999%, Alfa Aesar) was placed at the low temperature region. The temperature of the MoO_3 and sulfur zone was heated to 160 °C and 750 °C and kept for 10 min for growth of MoS_2.[16,17] After the reaction process, the furnace was cooled down to room temperature.

To fabricate the β-Ga_2O_3/MoS_2/Ce6 DUV and visible dual-band photodetectors, the as-synthesized MoS_2 was transferred onto the Ga_2O_3 film by a standard wetting transfer method.[18] Then, two Ti /Au electrodes with 100 nm in length, 50 nm in width, and 20 nm in spacing were prepared on the MoS_2 via photolithography and thermal evaporation. Last, Ce6 in aqueous solution (0.05 mg/ml) was coated onto the β-Ga_2O_3/MoS_2 substrate at 2000 rpm for 20 s to form the β-Ga_2O_3/MoS_2/Ce6 structure.

The structural properties of the Ga_2O_3 were investigated using x-ray diffraction (XRD). The absorption spectra of the Ga_2O_3 films and Ce6 were collected using a spectrophotometer (HITACHI, UH4150). The surface morphology was characterized using a field emission scanning electron microscope (FE-SEM, JSM-6700F/INCA-ENERGY). The photoelectric characteristics of the β-Ga_2O_3/MoS_2/Ce6 photodetector were measured using a semiconductor characterization system (Keithley 4200 SCS). The response spectra of the photodetector were performed using a photoresponse testing system with a 500-W xenon lamp as the light source, a monochromatic, a chopper and a lock-in amplifier.

3. Results and discussion

Figure 1(a) shows x-ray diffraction (XRD) pattern of the β-Ga_2O_3 films. There are three peaks located at 18.9°, 38.4°, and 59.2° corresponding to diffraction of the $(\bar{2}01)$, $(\bar{4}02)$, and $(\bar{6}03)$ planes of β-Ga_2O_3, respectively.[19,20] Scanning electron microscope (SEM) image suggests that the β-Ga_2O_3 is polycrystalline with an average grain size of about 300 nm, as presented in Fig. 1(b). Figure 1(c) shows the absorption spectrum of the β-Ga_2O_3, and an absorption edge at around 265 nm can be observed, indicating that the β-Ga_2O_3 is suitable for DUV detection.[21,22] Figure 1(d) displays the absorption spectrum (red curve) and photoluminescence (PL) spectrum (blue curve) of the Ce6, which shows an absorption (abs.) peak at around 403 nm and two weak absorption peaks at around 500 nm and 664 nm. These absorption peaks in the visible region suggest that Ce6 can be used for visible light detection.[13] The PL spectrum of the Ce6 with an emission peak at 662 nm, which proves that the luminescence of the Ce6 does not affect the optical response of the device. Figure 1(e) shows the SEM image of the Ce6. One can see that the size of the Ce6 clusters is in the range of dozens to hundreds nanometers. Figure 1(f) shows the SEM image of the MoS_2 multilayer which is a continuous membrane. The inset of Fig. 1(f) shows the SEM image of MoS_2 coated with Ce6, which displays that the MoS_2 is well covered by the Ce6 clusters.

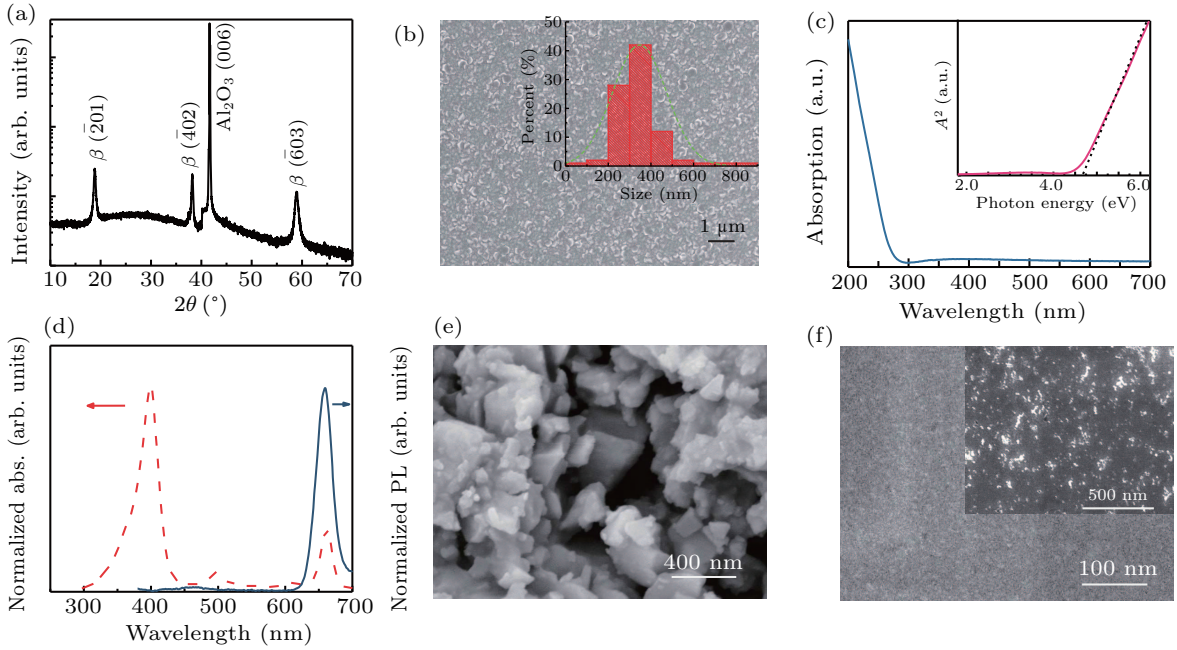


Fig. 1. (a) XRD pattern of the β-Ga_2O_3 films grown on sapphire. (b) SEM image of the β-Ga_2O_3 films; the inset shows the statistical results of the grain sizes. (c) Absorption spectrum of the β-Ga_2O_3 films; the inset shows the plot of absorption coefficient *versus* photon energy. (d) Absorption and PL spectra of the Ce6 dispersed in aqueous solution (0.05 mg/ml). (e) SEM image of the Ce6. (f) SEM image of the MoS_2 multilayer; the inset shows the SEM image of MoS_2 coated with Ce6.

Figure 2(a) shows the schematic diagram of the β-Ga_2O_3/MoS_2/Ce6 DUV and visible dual-band photodetector, in which the β-Ga_2O_3 and Ce6 act as the light absorption media, and MoS_2 as the photon-generated carrier collection layer.[14] The wavelength-dependent photoresponsivity of the β-Ga_2O_3/MoS_2/Ce6 photodetector is displayed in Fig. 2(b), which shows two separate peaks at 268 nm and 456 nm. Both of the two responsivity peaks increase with the applied voltage. When the applied voltage is 8 V, the responsivity at 268 nm and 456 nm reach 9.63 A/W and 1.17 A/W, respectively. The *I*–*V* characteristics of the β-Ga_2O_3/MoS_2/Ce6 photodetector under illumination of different wavelengths are investigated, as presented in Fig. 2(c). At 8-V bias, the photon currents under 254 nm and 450 nm is 3.9×10^{-5} A and 7.4×10^{-8} A, which are about four and two orders of magnitude larger than that under illumination of other wavelengths, respectively, confriming the response spectral selectivity.

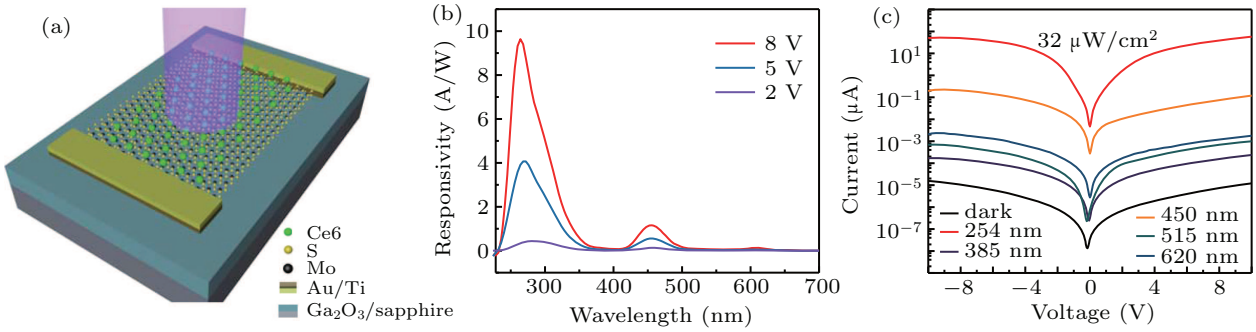


Fig. 2. (a) Schematic diagram of the β-Ga_2O_3/MoS_2/Ce6 photodetector. (b) Response spectra of β-Ga_2O_3/MoS_2/Ce6 photodetectors. (c) *I*–*V* characteristics of the β-Ga_2O_3/MoS_2/Ce6 photodetector in the dark and under illumination of different wavelengths.

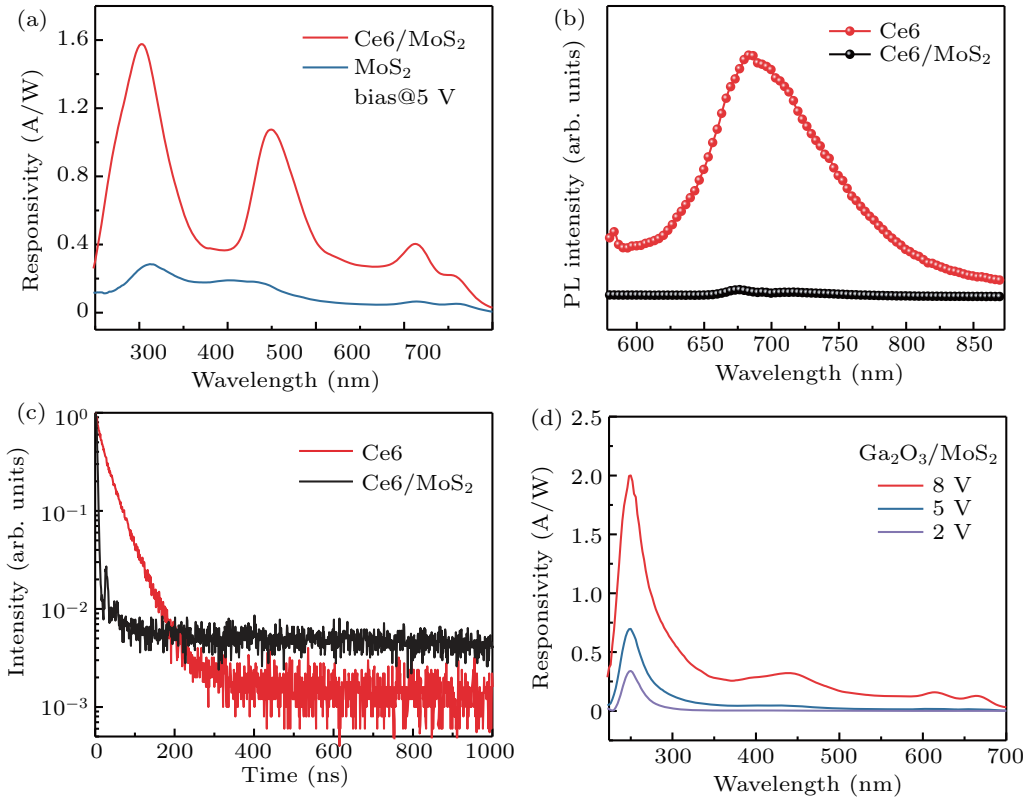


Fig. 3. (a) Photoresponse spectra of the MoS_2 (blue line) and Ce6/MoS_2 (red line) photodetectors. (b) PL spectra of the Ce6 and Ce6/MoS_2 on sapphire substrate. (c) Transient PL decay for Ce6 on sapphire substrate and Ce6-treated MoS_2 samples on sapphire substrate. (d) Response spectra of β-Ga_2O_3/MoS_2 photodetector.

To investigate the origin of the response peaks in the UV and visible regions, the photoresponse characteristics of β-Ga_2O_3/MoS_2 and MoS_2/Ce6 are investigated, as shown in Fig. 3. Figure 3(a) shows the photoresponse spectra of pristine MoS_2 (blue curve) and Ce6-coated MoS_2 (red curve) photodetectors at 5 V. The response spectrum of the MoS_2 exhibits four characteristic peaks located at 312, 440, 616, and 664 nm. The peaks at 616 nm and 664 nm can be attributed to the excitonic band edge transitions of MoS_2 from spin-degenerate valence bands to the conduction band near the *K*-point in the Brillouin zone.[23,24] The one at 440 nm can be assigned to the band nesting transition arising in a local-

ized region between K and G-points in the band structure of MoS_2.[25] The peak at 312 nm can be attributed to the wide absorption range of MoS_2.[23,24] Two distinct peaks located at about 300 nm and 450 nm can be observed from the response spectrum of the MoS_2/Ce6 photodetector. Compared with the pristine MoS_2 photodetector, the responsivity of the MoS_2/Ce6 photodetector has been enhanced, because the light absorption of the Ce6 is significantly higher than that of the MoS_2. Under illumination, the photon-generated electrons can be effectively transferred from the lowest unoccupied molecular orbit (LUMO) level of the Ce6 to the conduction band of the adjacent MoS_2.[1] Such electron transfer process increases the carrier concentration in the MoS_2, leading to the enhanced photocurrent.[26] However, compared with the absorption peak of the Ce6 at 403 nm, the visible responsitvity peak red-shifts by 53 nm due to the modulation of the adjacent MoS_2.[1] To further confirm the photon-generated carriers transfer process, PL characteristics of the pristine Ce6 and Ce6 on MoS_2 have been measured. As shown in Figs. 3(b) and 3(c), a quenching of PL of Ce6 on MoS_2 can be obtained. The PL lifetime is shortened from 14.2 μs for Ce6 in aqueous solution to 2.0 μs for Ce6 on MoS_2. The above results confirm the transfer of carriers from the Ce6 to the MoS_2, leading to enhanced responsivity in the visible region.[1,27,28] The response spectra of the Ga_2O_3/MoS_2 in Fig. 3(d) shows a strong response peak at 248 nm, and relatively weak peaks in the visible region. The peak in the DUV region can be attributed to the Ga_2O_3, and the peaks in the visible region can be attributed to MoS_2. Thus, by incorporating Ga_2O_3, Ce6, and MoS_2 in the β-Ga_2O_3/MoS_2/Ce6 structure, DUV and visible dual-band response can be achieved.

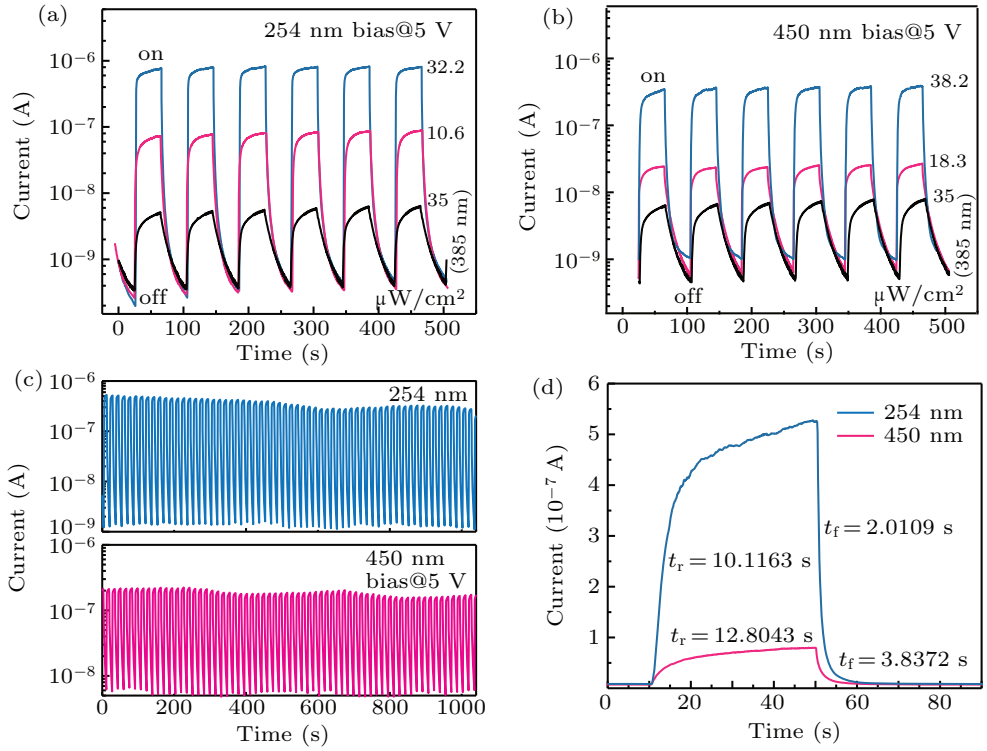


Fig. 4. The I–T curves of the device with periodical on/off switching upon 254 nm (a) and 450 nm (b) light under different light intensities. (c) The stability of the light current of the device. (d) Time response characteristics of the photodetector under 254-nm and 450-nm light illuminations.

Figures 4(a) and 4(b) show the time-resolved response under DUV (254 nm) and visible (450 nm) illumination, respectively, under the illumination of different light intensities. The photocurrent increases rapidly after the illumination is on and drops gradually after the illumination is off. The upward and downward trend stay at a stable I_{on}/I_{off} value of about 6.4×10^3 under DUV illumination (254 nm, 32.2 μW/cm^2). The photocurrent under visible illumination (450 nm, 38.2 μW/cm^2) also demonstrates a stable and reversible response with an I_{on}/I_{off} ratio of about 3.3×10^2. Moreover, under illumination with wavelength between the two photoresponse peaks (385 nm, 35 μW/cm^2), the photocurrent is about two order of magnitude smaller than that under 254-nm and 450-nm illuminations, further confirming the good response spectral selectivity. Figure 4(c) shows the continuous dark current and photocurrent of the β-Ga_2O_3/MoS_2/Ce6 photodetector with the illumination (254 nm and 450 nm) switched on and off for 64 cycles. The dark current and photocurrent of the photodetector are almost coincident, indicating the good stability and repeatability of the photodetector in both DUV and visible regions. Figure 4(d) shows response speed of the Ce6-modified photodetector by considering the 254-nm and 450-nm light as the excitation source. The rise time (time for the photocurrent

to increase from 10% to 90% of the maximum) is about 12.8 s under visible illumination and 10.1 s under UV illumination. Whereas the decay time (time for the photocurrent to decrease from 90% to 10% of the maximum) is about 3.8 s and 2.0 s, respectively.

4. Conclusions

In summary, we have demonstrated a DUV and visible dual-band photodetector by integration of Ga_2O_3 with Ce6 using a Ga_2O_3/MoS_2/Ce6 structure. The photodetector is highly spectral selective and shows two separate response bands at 268 nm and 456 nm, which can be attributed to transfer of photon-generated carriers from Ga_2O_3 and Ce6 to MoS_2. The response band in the DUV region has responsivity of 9.63 A/W with an FWHM of 54.5 nm; the response band in the visible region has a responsivity of 1.17 A/W with an FWHM of 45.3 nm. Our work may provide a applicable method for multi-band spectral selective photodetectors.

References

[1] Gao L, Ge C, Li W H, Jia C C, Zeng K, Pan W C, Wu H D, Zhao Y, He Y S, He J G, Zhao Z X, Niu G D, Guo X F, De Arquer F P G, Sargent E H and Tang J 2017 *Adv. Funct. Mater.* **27** 1702360

[2] Du S, Lu W, Ali A, *et al.* 2017 *Adv. Mater.* **29** 1700463

[3] Zhao J L, Yan L L, Chan W K E, Chen S M, Luo D and Zhu F R 2020 *Sci. Adv.* **6** eaaw8065

[4] Wu Y, Li X M, Wei Y, Gu Y and Zeng H B 2018 *Nanoscale* **10** 359

[5] Huang L J, Li J Q, Lu M Y, Chen Y Q, Zhu H J and Liu H Y 2020 *Chin. Phys. B* **29** 014201

[6] Zhang Y, Xu W X, Xu X J, Cai J, Yang W and Fang X S 2019 *J. Phys. Chem. Lett.* **10** 836

[7] Ariyawansa G, Apalkov V, Perera A G U, Matsik S G, Huang G and Bhattacharya P 2008 *Appl. Phys. Lett.* **92** 111104

[8] Hu R X, Ma X L, An C H and Liu J 2019 *Chin. Phys. B* **28** 117802

[9] Li K Y, Y X, Tian Y Z, Chen Y C, Lin C N, Zhang Z F, Xu Z Y, Zang J H and Shan C X 2020 *Sci. China-Phys. Mech. Astron.* **63** 117312

[10] Chu X L, Liu Z, Zhi Y S, Liu Y Y, Zhang S H, Wu C, Gao A, Li P G, Guo D Y, Wu Z P and Tang W H 2021 *Chin. Phys. B* **30** 017302

[11] Chen Y C, Lu Y J, Lin C N, Tian Y Z, Gao C J, Dong L and Shan C X 2018 *J. Mater. Chem. C* **6** 5727

[12] De Iacovo A, Venettacci C, Giansante C and Colace L 2020 *Nanoscale* **12** 10044

[13] Lightbourne S K S, Gobeze H B, Subbaiyan N K and D'souza F 2015 *J. Photon. Energy* **5** 053089

[14] Wang X F, Tamiaki H, Kitao O, Ikeuchi T and Sasaki S I 2013 *J. Power Sources* **242** 860

[15] Lin R, Zheng W, Zhang D, Zhang Z, Liao Q, Yang L and Huang F 2018 *ACS Appl. Mat. Interfaces* **10** 22419

[16] Huang Y, Zheng W, Qiu Y and Hu P 2016 *ACS Appl. Mater. Interfaces* **8** 23362

[17] Zhan Y, Liu Z, Najmaei S, Ajayan P M and Lou J 2012 *Small* **8** 966

[18] Wang J Z, Lu L, Lotya M, Coleman J N, Chou S L, Liu H K, Minett A I and Chen J 2013 *Adv. Energy Mater.* **3** 798

[19] Chen Y C, Lu Y J, Yang X, Li S F, Li K Y, Chen X X, Xu Z Y, Zang J H and Shan C X 2021 *Mater. Today Phys.* **18** 100369

[20] Guo X C, Hao N H, Guo D Y, Wu Z P, An Y H, Chu X L, Li L H, Li P G, Lei M and Tang W H 2016 *J. Alloys Compd.* **660** 136

[21] An Y H, Chu X L, Huang Y Q, Zhi Y S, Guo D Y, Li P G, Wu Z P and Tang W H 2016 *Prog. Nat. Sci.* **26** 65

[22] Feng Q, Li X, Han G Q, Huang L, Li F G, Tang W H, Zhang J C and Hao Y 2017 *Opt. Mater. Express* **7** 1240

[23] Lee S H, Park Y S, Yoo G W and Heo J S 2017 *Appl. Phys. Lett.* **111** 223106

[24] Mukherjee S, Maiti R, Midya A, Das S and Ray S K 2015 *ACS Photon.* **2** 760

[25] Aleithan S H, Livshits M Y, Khadka S, Rack J J, Kordesch M E and Stinaff E 2016 *Phys. Rev. B* **94** 035445

[26] Li S, Li G, Yang L S and Li K Y 2020 *Chin. Phys. B* **29** 046104

[27] Liu H, Gao F, Hu Y X, Zhang J, Wang L F, Feng W, Hou J and Hu P A 2019 *2D Mater.* **6** 035025

[28] Wu J 2021 *Chin. Phys. B* **30** 024208